MOUNTAIN-PLAINS CONSORTIUM

MPC 24-566 | Z. Yi and X. C. Liu

A MICROSCOPIC APPROACH FOR ELECTRIC VEHICLE DEMAND ESTIMATION

MOUNTAIN-PLAINS CONSORTIUM REGION 8

A University Transportation Center sponsored by the U.S. Department of Transportation serving the Mountain-Plains Region. Consortium members:

Colorado State University
North Dakota State University
South Dakota State University
University of Colorado Denver
University of Denver
University of Utah
Utah State University
University of Wyoming

Technical Report Documentation Page

1. Report No.	2. Government Accession No.	3. Recipient's Catalog No.
MPC-697		

4. Title and Subtitle	5. Report Date
A Microscopic Approach for Electric Vehicle Demand Estimation	October 2024
	6. Performing Organization Code

7. Author(s)	8. Performing Organization Report No.
Xiaoyue Cathy Liu Zhiyan Yi	MPC 24-566

9. Performing Organization Name and Address	10. Work Unit No. (TRAIS)
University of Utah 110 Central Campus Drive, Suie 2000 Salt Lake City, UT 84112	11. Contract or Grant No.

12. Sponsoring Agency Name and Address	13. Type of Report and Period Covered
Mountain-Plains Consortium North Dakota State University PO Box 6050, Fargo, ND 58108	Final Report
	14. Sponsoring Agency Code

15. Supplementary Notes

Supported by a grant from the US DOT, University Transportation Centers Program

16. Abstract

As the market penetration of electric vehicles (EVs) increases, the surge of charging demand could potentially overload the power grid and disrupt infrastructure planning. Hence, an efficient deployment strategy of electrical vehicle supply equipment (EVSE) is much needed. This project attempted to address the EVSE problem from a microscopic perspective by formulating the problem in two steps: public charging demand simulation and charging station location optimization. Specifically, we applied an agent-based modeling approach to produce high-resolution daily driving profiles within an urban-scale context using MATSim. Subsequently, we performed an EV assignment based on socioeconomic attributes to determine EV adopters. An energy consumption model and a public charging rule were specified for generating synthetic public charging demand, and such demand was validated against real-world public charging records to guarantee the robustness of simulation results. In the second step, we applied a location approach — the capacitated maximal coverage location problem (CMCLP) model — to reallocate existing charging stations with the objective of maximizing the coverage of total charging demands generated from the previous step under the budget and load capacity constraints. The entire framework is capable of modeling the spatiotemporal distribution of public charging demand in a bottom-up fashion, and provides practical support for future public EVSE installations.

17. Key Word	18. Distribution Statement
demand, electric vehicle charging, electric vehicles, optimization, simulation	Public distribution

19. Security Classif. (of this report)	20. Security Classif. (of this page)	21. No. of Pages	22. Price
Unclassified	Unclassified	42	n/a

A MICROSCOPIC APPROACH FOR ELECTRIC VEHICLE DEMAND ESTIMATION

Zhiyan Yi
Ph.D. Candidate
Department of Civil and Environmental Engineering
University of Utah
Salt Lake City, Utah, 84112
Email: zhiyan.yi@utah.edu

Xiaoyue Cathy Liu, Ph.D., P.E.
Associate Professor
Department of Civil and Environmental Engineering
University of Utah
Salt Lake City, Utah, 84112
Phone: (801) 587-8858
Email: cathy.liu@utah.edu

October 2024

Acknowledgements

The authors acknowledge the Mountain-Plains Consortium (MPC) and Global Energy Interconnection Research Institute North America (GEIRINA) for funding this research, and the following individuals for helping to guide the research and providing data to facilitate our modeling:

- Xi Chen (GEIRINA)
- Jiangpeng Dai (GEIRINA)
- James Campbell (Rocky Mountain Power)
- Regan Zane (Utah State University)

Disclaimer

ABSTRACT

As the market penetration of electric vehicles (EVs) increases, the surge of charging demand could potentially overload the power grid and disrupt infrastructure planning. Hence, an efficient deployment strategy of electrical vehicle supply equipment (EVSE) is much needed. This project attempted to address the EVSE problem from a microscopic perspective by formulating the problem in two steps: public charging demand simulation and charging station location optimization. Specifically, we applied an agent-based modeling approach to produce high-resolution daily driving profiles within an urban-scale context using MATSim. Subsequently, we performed an EV assignment based on socioeconomic attributes to determine EV adopters. An energy consumption model and a public charging rule were specified for generating synthetic public charging demand, and such demand was validated against real-world public charging records to guarantee the robustness of simulation results. In the second step, we applied a location approach — the capacitated maximal coverage location problem (CMCLP) model — to reallocate existing charging stations with the objective of maximizing the coverage of total charging demands generated from the previous step under the budget and load capacity constraints. The entire framework is capable of modeling the spatiotemporal distribution of public charging demand in a bottom-up fashion, and provides practical support for future public EVSE installations.

TABLE OF CONTENTS

LIST OF FIGURES

LIST OF TABLES

EXECUTIVE SUMMARY

This project aims to address the growing demand for public Electric Vehicle Supply Equipment (EVSE) by developing a microscopic approach for estimating electric vehicle (EV) charging demand and optimizing charging station locations in urban areas. With the increasing adoption of EVs, particularly in rapidly growing regions like the Salt Lake City (SLC) metropolitan area, efficient deployment of charging infrastructure is critical to avoid overloading the power grid and to meet the charging needs of EV users. The research was conducted in two phases. The first phase involved simulating public charging demand through an agent-based modeling approach using MATSim. The model synthesized high-resolution daily driving profiles based on sociodemographic attributes and historical trip data. EV assignment and energy consumption models were applied to determine the distribution of public charging demand. The second phase focused on optimizing the location of public charging stations using a capacitated maximal coverage location problem (CMCLP) model. This model reallocated existing charging stations while maximizing coverage of the charging demand, under constraints, such as investment cost and charging load capacity.

The major findings of the study revealed the optimized layout of charging stations significantly improved the overall performance of the public charging infrastructure. By using real-world charging data to validate the simulation results, the optimized network reduced the number of EV drivers with zero state-of-charge (SoC) by 20% and decreased the average charging time from 2.8 hours to 2.5 hours. Additionally, the model identified areas in the SLC metropolitan region with high charging demand but insufficient charging infrastructure, highlighting the need for strategic planning in expanding charging networks. This research has important implications for cities seeking to accelerate EV adoption while ensuring public charging infrastructure can meet future demand. The outcomes provide actionable insights for urban planners and policymakers, offering a scalable framework for optimizing public EVSE deployment to support sustainable transportation systems.

1. INTRODUCTION

1.1 Background

The electric vehicle (EV) market has been progressively growing in the past decade with promising sales records in many countries (Paoli & Gül, 2022). In the United States, for example, the sales of EVs and plug-in hybrid electric vehicles (PHEVs) nearly doubled from 308,000 in 2020 to 608,000 in 2021 (U.S. Department of Energy, 2022). In China, EV sales grew by 85% from 2018 to 2019, significantly above the industry average (McKinsey, 2019). Such significant rise in EV adoption rate is attributable to policy incentives, technological advancement, promotion of carbon neutral, and net-zero emissions economy, etc. (Debnath, Bardhan, Reiner, & Miller, 2021; Kumar, Chakraborty, & Mandal, 2021; Liu, Sun, Zheng, & Huang, 2021). The ever-increasing EV adoption is beneficial to reducing greenhouse gas (GHG) emissions, supporting the sustainable transport system, and decreasing the reliance on fossil fuels (Bor´en et al., 2017).

As the booming of EVs creates positive impacts in multiple areas, it also brings challenges to the entire society. Among those challenges is the surge of EV charging demand in response to the fast EV adoption, which could potentially overload the power grid and affect infrastructure planning (Deb, Kalita, & Mahanta, 2018; Deb, Tammi, Kalita, & Mahanta, 2018; Wu, Ravey, Chrenko, & Miraoui, 2019). EV charging can be divided into home charging and public charging, depending on charging locations. In the United States, home charging is still the dominant charging mode, accounting for approximately 80% of all charging events (Smart & Schey, 2012). However, public charging plays an indispensable role under several circumstances. First, drivers who often perform long-distance trips would heavily rely on public charging due to the limited mileage range of EVs. Second, home charging requires the charging facilities to be installed at a home garage. Yet many existing EV drivers or potential EV buyers may live in housing units that have no access to a garage or carport.

For instance, Ou, Lin, He, and Przesmitzki (2018) estimated that the home parking availability in Shanghai, China, was merely 5.3% in 2005. Therefore, augmenting the network coverage of public charging infrastructures can effectively eliminate the resistance to EV purchase. Last but not least, the concept of taxi electrification has been widely expanded in recent years as electric taxi pilots have already been launched in several cities, such as New York City and in Shenzhen, China (Yang, Dong, & Hu, 2018). Considering the much longer daily mileage of taxis, public charging infrastructures appear to be crucial to support such service.

A natural question to address, based on these aforementioned challenges, is how to optimally place public charging stations to increase demand coverage and sufficiently exploit utilization of the public electric vehicle supply equipment (EVSE). In general, EVSE location problems are often attempted in two steps: public charging demand estimation and public charging station location optimization. Through this workflow, the first step — how to accurately estimate public charging demand — is more challenging because the public charging decision is dictated by a myriad of complex factors, including drivers' charging preference, charging facility accessibility, and the EV's remaining state of charge (SoC) (Zhang, Luo, Qiu, & Fu, 2022). Previous studies on public charging demand estimation can be classified into macro- and micro-level approaches. For the macro-level studies, urban informatics and travel mobility information are often utilized to quantify public charging demand in different regions and to extract potential spatial correlation (Dong, Ma, Wei, & Haycox, 2019; Hu, Dong, Lin, & Yang, 2018; Kontou, Liu, Xie, Wu, & Lin, 2019; Tu et al., 2016; Vazifeh, Zhang, Santi, & Ratti, 2019; Yi, Liu, Wei, Chen, & Dai, 2021).

In contrast, micro-level approaches mimic EV drivers' daily travel behavior and public charging requests using simulation software in a bottom-up fashion (Adenaw & Lienkamp, 2021; He, Yin, & Zhou, 2015; Lopez, Allana, & Biona, 2021; Marmaras, Xydas, & Cipcigan, 2017; Novosel et al., 2015; Wang & Infield, 2018; Xi, Sioshansi, & Marano, 2013). Compared with macro-level approaches, micro-level methods are capable of producing high-resolution results, such as hourly-level charging distribution, for detailed behavioral analysis. Simulation tools can also model different charging scenarios (e.g., a mix of standard and fast charging events), in an attempt to manage the charging load. Moreover, simulation-based approaches can adopt future changes (e.g., the increase in EV adoption) when assessing the charging demand. For these reasons, micro-level approaches are more suitable to use if high-resolution constraints need be considered for optimizing charging infrastructures.
The majority of existing microscopic methods for public charging demand estimation follow a similar modeling framework, which can be roughly divided into three steps. The first step is to create synthetic drivers and assign them with daily driving profiles to simulate the traffic for the entire study area. This step can be achieved by either populating seed samples from household travel records or generating stochastic activities using Markov chain (Wang, Huang, & Infield, 2014; Xi et al., 2013). The subsequent step is to assign EV drivers that match the current EV adoption rate and its spatial distribution. The final step is to specify EVs' energy consumption model and the public charging decision rule to produce synthetic public charging demands.

Although previous studies, in general, follow such modeling steps, there are many oversimplified assumptions and/or limitations that prevent the model from reproducing accurate spatiotemporal public charging demand portfolios, especially for large-scale (e.g. urban-scale) simulations. Small road networks or simplified network topologies are commonly used for exploring public charging demand considering computational expensiveness (He et al., 2015; Marmaras et al., 2017; Wang & Infield, 2018). However, conclusions from those studies might not be applicable to city-scale analyses, since real traffic patterns vary significantly across geographical areas and interact in a complex manner. Besides, oversimplification of EV assignment and public charging decision rules can lead to biased estimation of the total energy demand. Several studies assumed a uniform distribution with a fixed EV penetration rate to create synthetic EV drivers (Khan, Mehmood, Haider, Rafique, & Kim, 2018; Wang & Infield, 2018). Yet, the decision of EV adoption is driven by miscellaneous factors, including EV model (e.g. mileage range), socio-demographic characteristics (e.g. income, age), and context variables (e.g. accessibility to charging equipment and fuel price) (Javid & Nejat, 2017). Therefore, assumption of random distributions could overlook heterogeneities across neighborhoods and individuals.

Apart from EV assignment, simplifying daily activities by confining them to only work-based and/or home-based activities in simulation is another limitation (Lopez et al., 2021; Novosel et al., 2015). Places associated with non-work-based activities, such as shopping malls, restaurants, entertainment locations, and airports, also demonstrate potential public charging needs (Nansai, Tohno, Kono, Kasahara, & Moriguchi, 2001). More importantly, most previous studies were not validated against real-world public charging records, leading to over/under-estimation of the actual public charging demand and inaccurate spatiotemporal charging distribution evaluation. The major hurdle in obtaining public charging data is commercial and/or governmental confidentialities (Wang & Ke, 2018). Without the support of real-world public charging records, the subsequent charging station optimization process would render less meaningful.

1.2 Objectives

This study aims to optimize the layout of public charging stations at the city-scale by addressing the following two overarching research questions:

- How to link potential EV users' daily activity patterns with their charging behavior and further estimate the spatial distribution of public charging demand?
- Once an estimated charging demand distribution is accomplished, how to optimize the layout of public charging stations such that the overall public charging demand is maximized?

Specifically, the Salt Lake City (SLC) metropolitan area was selected as a pilot. Utah is the fourth fastest growing state in the United States, and its population is forecasted to double over the next 20 years. The SLC metropolitan area is home to >80% of the state's population and, surprisingly, experiences some of the worst air quality in the nation. As such, there is growing political consensus to address air quality, and PEVs offer a viable solution. The state has aggressive plan in terms of charging station deployment over the next several years and understanding how drivers' daily activities interact with public charging demand at city-scale is paramount to the EV charging station deployment. Therefore, the modeling framework and findings could provide valuable guidance to regions or areas with similar interests in accelerating EV adoption. As for the modeling process, we first create the synthetic public charging demand within an urban-scale context in a bottom-up fashion via agent-based modeling. Specifically, Multi-agent Transport Simulation (MATSim), an open-source framework for implementing large-scale agent-based transport simulation, is adopted to model the daily activities of all drivers. Then, we distributed the EV drivers based on socioeconomic attributes, and further, specified the public charging decision rule for generating synthetic public charging demand post-simulation. In the second step, an optimization framework — capacitated maximal coverage location problem (CMCLP) — was formulated based on the generated public charging demands from the previous step. The CMCLP model reallocated existing public charging stations in the study area by maximizing the coverage of total charging demand under the investment cost and load capacity constraints. Note that within the entire framework, synthetic public charging demand was validated against real-world charging records, and optimized charging station deployment was assessed by a plug-in from MATSim that supports the public charging behavior analysis.

In sum, the main contributions of this research were threefold:

- A city-scale agent-based simulation was developed to produce daily travel profiles using time-inhomogeneous Markov chain, and location mapping technique using publicly available data. EV assignment and public charging decision modeling were subsequently specified in post-simulation analyses using socioeconomic and demographic information to produce high-resolution public charging demand.
- The spatiotemporal distribution of synthetic charging demand was validated against real-world public charging records, which are obtained using a dynamic crawling pipeline. The result indicated a consistent charging pattern between synthetic charging demand and actual energy consumption for most areas.
- The CMCLP model was applied to optimize the deployment of public charging stations taking into consideration both standard and fast charging demands. The capacity constraint was formulated at different hours-of-the-day to ensure charging demands were satisfied even during peak hours. The results can provide practical guidance for future public EVSE installation.

1.3 Outline of Report

The rest of the report is structured as follows. Chapter 2 comprehensively discusses literature related to simulation-based public charging demand analyses, agent-based modeling, and charging station locations optimization problems. Chapter 3 describes data sources in detail. Chapter 4 presents the micro-level modeling framework for public charging demand generation and mathematical formulation of CMCLP model. Chapter 5 presents the simulation results, charging demand analyses, and optimization outcomes. And research conclusions are outlined in Chapter 6.

2. LITERATURE REVIEW

2.1 Simulation-based Public Charging Demand Modeling

Microscopic simulation-based approaches model the public charging demand generation in a bottom-up fashion. One of their major advantages is the ability to reproduce complex traffic situations within large-scale networks and enable operational outputs at the link or intersection level while accounting for the impacts of localized activities. Microscopic modeling produces detailed trip trajectory at the individual level, which can be used for high-resolution analysis. Moreover, the animation and graphic user interface allow researchers to vividly interpret the impact of drivers' daily activities on public charging behavior. In general, simulation-based approaches for generating public charging demand follow three steps: simulating the daily traffic for the entire study area, assigning EVs among drivers, and specifying energy consumption model and public charging decision rules.

The first step can be achieved using simulation software, while the remaining steps can be performed as post-simulation analysis. To model daily traffic, all drivers' household distribution and their daily driving profiles are required. This process can be further separated into population synthesis and stochastic daily activity generation. Population synthesis refers to the use of sample population data to generate a set of households and persons representing the entire population in the modeling region (Paul, Doyle, Stabler, Freedman, & Bettinardi, 2018). Marginal distributions of socioeconomic and demographic characteristics are fed into a population synthesizer with the sample data to create heterogeneous households and individuals.

As for stochastic daily activity generation, a common approach is to apply Markov Chain Monte Carlo (MCMC) simulation. For example, Wang et al. (2014) applied a time-inhomogeneous Markov chain to simulate driving patterns based on the UK 2000 Time Use Survey data, a real-world high-resolution dataset that records activities for households' individuals on a 10-minute basis. Four states including “driving,” “parking at home,” “parking at workplace,” and “parking at other places” are defined in the Markov chain for the privately owned EVs to estimate the impact of workplace charging during weekday on power grid. Once the synthetic population and their daily activity trips are generated, simulation software can be used to model the traffic of study area with road network information. Following that, a post-simulation analysis can be conducted to assign EV users and distribute public charging demands according to a specified charging decision.

A simple strategy for EV assignment is to distribute EV drivers using uniform distribution with a fixed EV penetration rate ranging from 1% to 100% (Khan et al., 2018; Wang & Infield, 2018; Xi et al., 2013). However, EV adoption is influenced by a myriad of factors, including demographic, contextual, and other types of attributes. The assumption of uniform distribution would ignore the socioeconomic and demographic distinctions across geographical areas, leading to biased EV adoption spread and incorrect charging demand distribution. To estimate EV adoption probability, Javid and Nejat (2017) developed a logistic regression model that considers socioeconomic factors and context variables, such as age, income, and fuel price. After EV assignment, energy consumption model and public charging decision behaviors should be established to determine when and where public charging events occur. The public charging decision rule is relatively difficult to model since drivers' charging preference, charging accessibility, and remaining SoC are challenging to be captured precisely (Herberz, Hahnel, & Brosch, 2022).

In previous studies, the attributing factors for modeling public charging include SoC, activity duration, and walking distance to the charging facilities. Researchers generally set a threshold value for each factor according to published reports to trigger public charging events with different logics (Hu et al., 2018; Wang et al., 2014; Zou, Wei, Sun, Hu, & Shiao, 2016). After performing the aforementioned three steps (daily traffic simulation, EV assignment, and energy consumption and charging decision), the generated synthetic public charging demands can be represented using points. Each demand point is associated with a charging start time, duration, charging type, and location information. This information will be further utilized in the optimization framework for optimizing the public charging station locations.

2.2 Agent-based Modeling

Note that there are multiple ways for conducting daily traffic simulation based on the synthetic population and their daily activity trips. Among them, agent-based model (ABM) is one of the widely used approaches. ABM contains a collection of agents or units, and agents can be assigned with different daily activities. The agents will operate according to plans and interact mutually to produce a complex scenario, such as road traffic (Macal & North, 2009). ABM provides a natural description of a system that is highly flexible. It enables the creation of complex simulation environments by inserting heterogeneous units with a variety of attributes, such as age, vocation, and income level. Popular agent-based modeling tools for traffic analysis include Transportation Analysis Simulation System (TRANSIMS) (Smith, Beckman, & Baggerly, 1995), Simulation of Urban Mobility (SUMO) (Krajzewicz, Erdmann, Behrisch, & Bieker, 2012), and MATSim (Axhausen, Horni, & Nagel, 2016). MATSim is an open-source framework for implementing large-scale agent-based transport simulations. It is arguably the one with the least focus on traffic flow realism but with the highest computing speed and the best behavior model on trip planning. In a nutshell, a synthetic driver (i.e. agent) will perform trip activities within a day and try its best to optimize its daily schedule by adjusting possible activities based on a co-evolutionary principle iteratively.

Because MATSim is written in Java, it supports a variety of plug-in packages for public charging behavior analyses (e.g. BEAM and DVRP) (Maciejewski & Nagal, 2007; Sheppard, Waraich, Campbell, Pozdnukov, & Gopal, 2017). MATSim requires population distribution, daily activities, road network, and facility locations as inputs. Novosel et al. (2015) applied MATSim to model the hourly distribution of energy consumption of EVs on an urban scale in the cities of Croatia to test their charging impacts on the entire energy system. This study assumed activities only occured between home and work, and the spatial distribution of home and work locations were estimated based on the socio-demographic data. Adenaw and Lienkamp (2021) applied MATSim to analyze the charging station utilization and user behavior by inserting EVs and charging stations in the simulation environment. The numeric results were tested and verified using a case study in the city of Munich, reflecting realistic spatiotemporal charging patterns. Furthermore, they encapsulated their work to an open-source framework – UrbanEv-Contrib – based on MATSim, which can serve as a sandbox validating optimized charging infrastructure designs in a dynamic simulation environment.

2.3 Public Charging Station Locations Optimization

Public charging infrastructure deployment problems can be solved using location approaches, which contain two components: demand representation and location model. Charging demand can be represented as points, polygons, or flows, depending on the specific contexts, and the location model is an optimization framework designed to select the best locations with the goal of maximum utility coverage, minimum cost, or other objectives (Dong et al., 2019; Huang, Kanaroglou, & Zhang, 2016). Demand is considered being covered if it is within a certain travel distance to a charging station. Standard location models include the flow capture location model (FCLM) (Hodgson, 1990), maximal coverage location problem (MCLP) (Church & ReVelle, 1974), and p-Center (Hakimi, 1964). Among them, the MCLP model is computationally efficient and suitable for problems with demand representation as points or polygons. The MCLP seeks to maximize the target (i.e. charging demand) covered within a desired service distance by locating a fixed number of facilities (i.e. public charging stations). It has been widely adopted for solving the EVSE location problem. Dong et al. (2019) optimized the placement of charge point infrastructure by formulating a MCLP model with the objective of maximizing total demand coverage under the investment budget constraint.

One potential flaw of the MCLP model is that the energy capacity for charging ports is not considered. Failing to set capacity limits can lead to an overestimation of service level. To fix this problem, the CMCLP model is developed to refine constraints. Yi, Liu, and Wei (2022) utilized the CMCLP model to optimize the layout of public charging stations on a city scale. Accumulated daily capacity for each charging port and total investment budgets are set as constraints. With finer granularity, hourly charging capacity can be modeled to satisfy the charging demand during peak hours (Tu et al., 2016). The aforementioned MCLP/CMCLP-based charging station optimization models (Asamer, Reinthaler, Ruthmair, Straub, & Puchinger, 2016; Dong et al., 2019; Tu et al., 2016; Yi et al., 2022) attempted the problem from a macro-level, where the entire study area is discretized into grids or polygons, and charging stations are sited onto those cells instead of pinpointed to the exact geographical locations. Such discretization will induce low-resolution optimization results because the size of cells can be as large as 1 km by 1 km (Yi et al., 2022). Failing to pinpoint the exact location of charging facilities might provide less practical or useful guidance for detailed infrastructure planning. The ABM can effectively address this problem as it is capable of producing vehicle trajectory records and high-resolution charging requests. Our study employed CMCLP to maximally capture the public charging demands in the study area under the investment budget and different hours-of-day capacity constraints. Moreover, fast charging demand was incorporated on top of standard charging demand in the optimization framework to present a more realistic charging infrastructure design.

3. DATA

A realistic urban-scale simulation requires high-quality inputs. The modeling framework presented in Figure 3.1 consists of a series of building blocks. In each building block, methodology (will be explained in the next section) and required data resources are highlighted. First, population and socioeconomic attributes were used for synthetic population generation, and ATUS data was utilized to create time-inhomogeneous Markov chain. Following that, POI and historical OD data were used for location mapping. To execute agent-based simulation via MATSim, road network information was fetched from Open Street Map (OSM). EV assignment and public charging behavior modeling were subsequently performed. Finally, real-world public charging observations were used to validate simulation results, while an optimization model was further implemented based on the simulation results to reallocate the charging stations with maximum coverage of public charging demands. The detailed description for each dataset is explained in the following subsections.

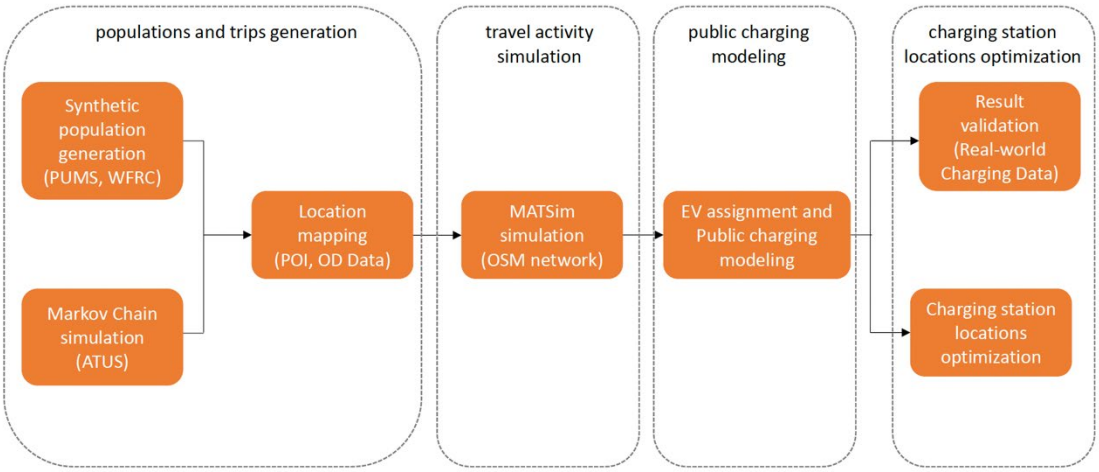

Figure 3.1 Model development framework

3.1 American Time Use Survey (ATUS)

High quality data is essential to guarantee accurate stochastic behavior modeling for agent-based simulation. Time use survey data has been widely used to model stochastic behaviors of people due to the high resolution of activity information. Hence, we employed ATUS dataset to create synthetic agents. ATUS dataset is collected annually by U.S. Bureau of Labor Statistics, which provides nationally representative estimates of how, where, and with whom people spend their time. Each respondent interviewed by ATUS is documented with demographic information, household status, and daily activity records. To reflect how people spend their time, respondents are asked to collect a detailed account of their activities regarding the type, duration, and location of activities, starting at 4:00 AM the previous day and ending at 4:00 AM on the interview day. We used ATUS data spanning from 2013 to 2017 with approximately 55,000 respondents during weekdays to construct the Markov chain for stochastic daily activities generation.

3.2 OSM Road Network Information

We extracted road network using OSMnx, a python package allowing to download, visualize, and analyze geospatial data from OSM as the required input for MATSim (Boeing, 2017). The representation of a road network in OSM is essentially a directed graph, where edges represent roads and nodes represent conjunction points or dead end of roads. Each road contains the topological information such as coordinates of start and end point, the line string geometry, and length. Moreover, each road is assigned with traffic attributes, such as road class, number of lanes, and maximum speed, which are required attributes for MATSim. There are 94,742 roads and 37,766 conjunction points (or dead ends) in total within study area. Roads attributes with missing values are replaced by mean values of all roads within the same road class.

3.3 Sociodemographic Information

Synthetic population generation requires two inputs — sample seed and attributes' marginal distributions — to create an entire population in the study region. A population sample from Public Use Microdata Sample (PUMS), which is a set of records from individual people or household units with disclosure protection enabled (United States Census Bureau, 2019), was used as sample seed. There were 4,924 households and 13,768 persons in the seed population. Each sample household contained attributes, including household size, household income, vehicle ownership, and location information. Apart from sample seed, marginal distributions of the aforementioned attributes were required. This study applies TAZ-level socio-demographical information with fine granularity to create realistic simulation scenario. Household distribution, vehicle ownership and average household income in each TAZ are retrieved from Wasatch Front Regional Council (WFRC) to build the marginal distributions of sample's attributes at TAZ level (Wasatch Front Regional Council, 2021). Historical OD distribution data among TAZs also was used for location mapping purpose.

3.4 Point of Interest (POI) Data

POI data can effectively reflect urban context and infer people's trip purposes. To extract POIs in our study area, we used Google Place API (Google Place API, 2021). After eliminating unrelated type of POIs (e.g. hotel), there were 59,112 POIs classified in nine categories. The detailed information of classified POI data is shown in Table 3.1. The POI information was retrieved for the location mapping purpose. Each category of POIs was associated with a specific daily activity as observed in the Activity column.

Table 3.1 Description of POI data

POI ID	Category	Label Examples	Count	Activity
1	Business	office, personal business	23,472	Work
2	Health	hospital, health, doctor	8,982	Others
3	Finance	agency, finance building	6,691	Work
4	Retail	supermarket, grocery store	10,066	Shop
5	Restaurant	restaurant, food delivery	2,181	Dine in
6	Education	school, university	1,290	Others
7	NGO	church, government building	1,591	Work
8	Entertainments	park, salon, bar, zoo	2,422	Others
9	Service	post office, gas station, laundry	2,427	Others

3.5 Real-world Public Charging Data

The real-world charging data was crawled from ChargePoint, an online application that assists EV users to navigate and review nearby charging sites (Charge Point, 2021). ChargePoint operates the largest online network of independently owned EV charging stations, operating in 14 countries worldwide. The data crawling period spanned from November 5, 2020, to December 12, 2020, and the construction steps for dynamic crawling pipeline can be found in (Yi et al., 2022). To sum, there are 109 public charging stations with 516 Level 2 charging ports recorded by ChargePoint that broadcast real-time utilization information (i.e., number of in-use ports at current time point) in the study area. The energy consumption at a certain period for a charging station is calculated as the total number of in-use ports multiplied by the corresponding power of the ports and crawling interval (set as 10 minutes). The accumulative energy consumption (kWh) during each interval is then summed up across the entire crawling period as the total charging energy consumption. Spatial distribution for 109 charging stations is displayed in Figure 3.2, with the height quantifying the cumulative energy consumption within the data collection period.

Figure 3.2 The spatial distribution of current public charging stations in Salt Lake City metropolitan area

4. MODELING FRAMEWORK

To simulate EV mobility and associated energy consumption in a high-spatiotemporal resolution, the modeling framework in Figure 3.1 was divided into four major components: populations and trips generation; travel activity simulation; public charging modeling; and charging station location optimization. We began by creating a synthetic population using sociodemographic information at the traffic analysis zone (TAZ) level. In the meantime, a time-inhomogeneous Markov chain was trained using ATUS data to produce stochastic daily activities. Following that, a location mapping technique was proposed to project those daily activities onto specific geographical locations based on historical travel patterns, POI, and population information. These aforementioned inputs were then fed into MATSim, together with road network, to return the optimal travel plans for all drivers. Upon MATSim simulation result, we applied the EV adoption probability model and EV energy consumption model to determine EV distribution and potential public charging demands. This was validated against real-world public charging observations. An optimization model was then employed to maximize the coverage of public charging demand under various constraints.

4.1 Synthetic Population Generation

Synthetic population generation is the first step of activity-based modeling. The generated synthetic population should represent person- and/or household-level attributes of the actual population in the modeling region. PopulationSim (Paul et al., 2018), an open-source population synthesizer, was employed for the purpose of this study. Typically, PopulationSim requires three datasets as the inputs: household and person samples with related sociodemographic attributes, and the marginal distributions of controlled variables (e.g., household size and household income). Then PopulationSim utilizes the samples and marginal distributions to generate tables of person and households representing the entire population of the modeling region.

The population synthesis in PopulationSim involves two steps: fitting and generation. During the fitting step, entropy maximization is applied to preserve the distribution of initial weights while matching the marginal controls. Once the weights have been assigned for seed sample, the generation step expands the sample using Monte Carlo sampling and optimization-based algorithm. Table 4.1 gives an example of input data for PopluationSim, comprising the population sample (household and person), and marginal distributions of household size (HHSize), household income (HHInc), and household vehicle ownership (HHVeh) in TAZs. Note that the population sample data in PUMS was aggregated by public use microdata areas (PUMAs) — the special nonoverlapping areas that partition each state into contiguous geographic units containing no fewer than 100,000 people each, to protect privacy. PopulationSim allows reallocation of population from a larger geographic unit into a smaller one, such as from PUMAs to TAZs. The final outputs from PopulationSim contain synthetic populations and households with corresponding attributes at located TAZs in the study region.

Table 4.1 Sample input data for PopulationSim

(a) Population sample at PUMA level

Household id	PUMA id	HHSize	HHInc	HHVeh
1	35001	2	50000	2

Person id	Household id	PUMA id	Age	Gender
1-1	1	35001	51	male
1-2	1	35001	46	female

(b) Marginal distributions of controlled variables in TAZs

TAZ id	695	712
PUMA id	35001	35001
Categories of HHSize		
HHSize = 1	174	97
HHSize = 2	109	137
HHSize = 3	75	221
HHSize = 4	34	220
HHSize = 5	105	22
HHSize = 6	86	125
HHSize ≥ 7	75	219
Categories of HHInc		
HHInc ≤ 21297	41	161
21297 < HHInc ≤ 42593	56	55
42593 < HHInc ≤ 85185	19	47
HHInc > 85185	10	46
Categories of HHVeh		
HHVeh = 0	19	12
HHVeh = 1	115	110
HHVeh = 2	161	329
HHVeh ≥ 3	97	224

4.2 Time-inhomogeneous Markov Chain

Vehicle movement is a series of state transitions throughout a day. The Markov chain is a stochastic model describing a sequence of possible events. Time-inhomogeneous Markov chain refers to chains with different transition probability matrices at each time step. In this study, ATUS data was utilized to construct the sequence of transition matrices for time-inhomogeneous Markov chain. We set time resolution as 10 minutes (i.e., 144 time steps for an entire day) when using a discrete Markov chain to describe people's daily activities. Such resolution is preferred for detailed analysis of vehicle activities and trips of short distances (Wang et al., 2014). Specifically, drivers' daily activities are classified into six categories: "drive," "stay home," "work," "shop," "dine in," and "others." The indexed activities and state transition relationship are described in Figure 4.1(a). Figure 4.1(b) describes the transition probability at a specific time t. For example, if $t = 48$, then p_{0248} denotes the probability from "drive" to "work" at 8:00 AM. Note that the transition between any two different states must be accomplished via "driving" activity, which means the transition probability between two nondriving states, such as p_{21t}, is always zero. This assumption was made because we were only interested in the activities that are connected by driving to explore EVs' potential charging opportunities at different locations.

To demonstrate the functionality of this Markov chain, each respondent's daily activity trajectory was first mapped to the state code in Figure 4.1(a), and then subsequently transformed to a list representation with the length of 144, where each number in the list denoted an activity code (10-minute resolution) at a specific time step. The transition probability p_{ijt}in stochastic matrix at time step t was calculated as the number of respondents switching from activity i to j at time step t + 1 divided by the total number of respondents. Once 143 stochastic matrices (a daily activity list contains 144 time steps) were obtained, we could use them to create a list of synthetic daily activities given the initial states as inputs. The initial state (i.e. activity at 12:00 am) for each person was determined by randomly sampling from a predefined probability density function at $t = 1$.

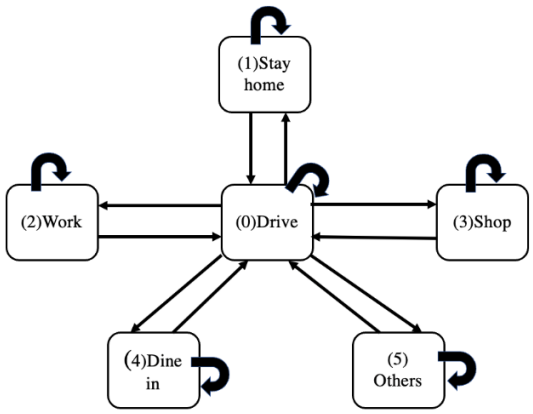

(a) Markov chain diagram of state transition

$$T_t = \begin{bmatrix} P_{00}^t & P_{01}^t & P_{02}^t & P_{03}^t & P_{04}^t & P_{05}^t \\ P_{10}^t & P_{11}^t & P_{12}^t & P_{13}^t & P_{14}^t & P_{15}^t \\ P_{20}^t & P_{21}^t & P_{22}^t & P_{23}^t & P_{24}^t & P_{25}^t \\ P_{30}^t & P_{31}^t & P_{32}^t & P_{33}^t & P_{34}^t & P_{35}^t \\ P_{40}^t & P_{41}^t & P_{42}^t & P_{43}^t & P_{44}^t & P_{45}^t \\ P_{50}^t & P_{51}^t & P_{52}^t & P_{53}^t & P_{54}^t & P_{55}^t \end{bmatrix}$$

(b) Transition matrix at time *t*

Figure 4.1 The Time-inhomogeneous Markov chain at time *t*

4.3 Location Mapping

Stochastic activities generated by Markov chain do not have geographical location information. Yet, ABMs, such as MATSim, require detailed trip information. Therefore, we developed a location mapping strategy to project abstract activities to specific trips with geo-location labels using historical trip distribution and POI data. The proposed location mapping strategy is detailed as follows:

- Search candidate TAZs: We searched TAZs that a driver could reach within a time threshold. Specifically, for any daily activities, we set the lower bound and upper bound of arrival time. If the driver arrived at the centroid of a TAZ within the time-boundary, the TAZ fell into the candidate set. We empirically set 0.8tdrive and 1.2tdrive as the lower bound and upper bound, respectively, where *t*drive is the driving time generated by Markov chain, which is formally defined as the number of continuous driving states multiplied by the time resolution of the Markov chain.
- Determine the exact destination TAZ: Once candidate TAZs were identified, we utilized historical OD distribution probability from the start TAZ to all candidate TAZs to determine at which TAZ the trip arrived. To achieve this, OD data for a typical workday was divided into four subsets time periods (i.e., 12:00 am – 6:00 am, 6:00 am – 12:00 pm, 12:00 pm – 6:00 pm, and 6:00 pm – 12:00 am). Trip counts from the source TAZ to candidate TAZs were fetched from one of the subsets depending on the activity start time. The probability that a trip arrived at any candidate TAZ was proportional to the trip count from the source TAZ to that TAZ divided by trip counts to all candidate TAZs. The OD data was split by time periods because many activities possessed strong temporal patterns, such as work-based trips.

- Pinpoint trip destination: After the destination TAZ was determined, we randomly assigned one POI with a corresponding trip purpose as the activity destination in the determined TAZ. For instance, if the activity purpose was "dine-in," we chose one POI with the label "restaurant." The mapping between activity purpose and POI label can be found in Section 3.4 *POI data.*

Since each daily activity could contain multiple intermediate stops, the location mapping process is iterated starting from home until the last activity is completed. Note that if location mapping fails to capture any intermediary stops for some reason (e.g. long driving duration), this activity would be discarded from the system.

4.4 EV Assignment and Energy Consumption Model

MATSim was used to simulate all vehicles' daily trips within a study region. As post-simulation analysis, we performed EV assignment and set up public charging rules to determine public charging demand distribution. For the EV assignment, we applied the EV adoption probability model developed by Javid and Nejat (2017). Javid and Nejat (2017), a logit model using the California Statewide Travel Survey data, and validated it against another dataset in Delaware, Texas. The result showed robust transferability in terms of the Area Under the Curve (AUC) — a classic metric for classification models. Therefore, we adopted the model here to assign EV drivers in the study region. The mathematical formulation is presented as follows:

$$\mathrm{p(x)} = \frac{1}{1+e^{-(\sum \alpha_i * x_i + \beta)}} \quad (1)$$

where *x* represents an individual that could potentially become an EV driver in a household, *xi* denotes internal or external factor that influences the purchase decision of individual *x*, and *αi* is the corresponding coefficient. p(x) is the estimated EV adoption probability for individual *x*. Eq. (1) is a logit model considering socioeconomic and demographic features. Table 4.2 lists the values of the variables and corresponding coefficients used. Individuals' attributes, including age, income, vehicle ownership, and household size, are used to calculate the EV adoption probabilities. Variables with minor variations across regions or those difficult to obtain, such as gas price and education level, were set as constants for simplicity. Note that constant values (excluding x_{gas_price} and x_{elec_price}) and coefficients are referenced from (Javid & Nejat, 2017). Public charging is a stochastic process.

Most charging mechanisms are based on the state of charge (SoC) or equivalent range anxiety (Hu et al., 2018; Wang et al., 2014). In this study, two types of charging were considered — standard charging (Level 2) and fast charging (Level 3). SoC was updated for each trip once the driver arrives at the next destination. Charging behavior was determined by the current SoC and dwell time. A flowchart with explicit charging rules is presented in Figure 4.2. The proposed charging rules considered three charging behaviors: no charging, standard charging, and fast charging. According to Zou et al. (2016), over 75% EV drivers will not charge their vehicles unless SoC drops below 50%. For this reason, we assumed EV drivers would consider public charging only when SoC is below 50%. When SoC drops below 50%, EV drivers may conduct Level 2 charging. However, drivers may refuse to charge if the dwell time *D* is too short. Hence, 30 minutes of minimal charging time was used to determine the Level 2 charging preference (Yi & Bauer, 2016). However, if SoC dropped below 15%, the EV driver would opt for fast charging, regardless of the dwell time.

Besides charging rules, the initial SoC should be determined. In fact, not all EV drivers have access to home charging equipment, and overnight charging might not be necessarily performed. The assumption of fully charged batteries before drivers depart home is not practical. Instead, the initial SoCs was generated from a normal distribution (Zheng, Wang, Men, Zhu, & Zhu, 2013). It is worthy to mention that the aforementioned charging rules only produced charging requests (or demands). It does not imply that charging is fulfilled at that moment, since public charging stations may or may not exist nearby for each charging request. The actual charging fulfillment will be discussed in optimization analyses.

Table 4.2 Variables and coefficients in EV adoption probability model

Variable	Coefficient	Explanation	Constant
x_{age}	0.04	Driver's age	NA
x_{car_share}	0.911	Weather the vehicle is shared with other drivers	0.01
x_{trip_dur}	0.001	Average daily trip duration (miles)	52.4
x_{income_level}	0.461	Categorized variable indicating the level of income with 1 denoting the lowest and 5 denoting the highest income	NA
$x_{household}$	-0.071	Categorized variable indicating the size of household	NA
$x_{education}$	0.274	Categorized variable indicating the education level	4.76
$x_{station\_num}$	0.811	Charging station per capita	0.5
x_{gas_price}	2.8	The gas price (dollar/gallon)	3.6
x_{elec_price}	0.077	The electricity price per (cent/kWh)	14.6
x_{veh_num}	-0.055	The number of vehicles owned by the driver	NA
β	-19.629	Constant term	NA

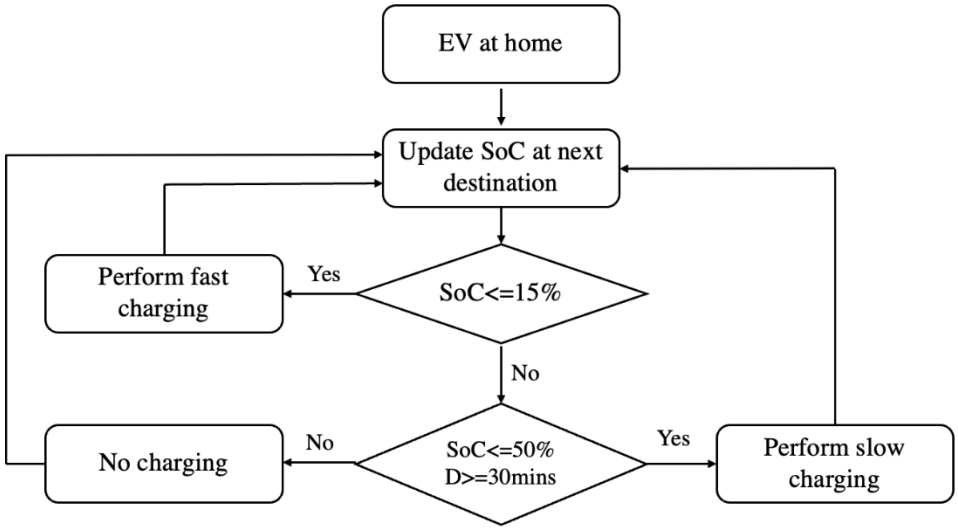

Figure 4.2 Rules for EV charging

4.5 CMCLP Optimization Model

We consider both standard charging and fast charging. Table 4.3 and Table 4.4 give the description of input parameters and decision variables for CMCLP model, separately. The objective of CMCLP is to maximize the coverage of public charging demands under a variety of constraints, including charging capacity, access distance, and investment budget. For charging capacity, it is applied by different hours-of-the-day to consider surging demands during peak hours. To formulate the hours-of-the-day constraints for charging stations, charging demands (i. e., charging request) were discretized. For instance, if a public charging event was performed between 8:00 AM and 10:45 AM, it was first rounded to a 3-hour request (from 8:00 AM – 11:00 AM) and discretized by hour – 8:00 AM-9:00 AM, 9:00 AM-10:00 AM, and 10:00 AM-11:00 AM. The charging demands were determined by the proposed charging rules in Figure 4.2, while the energy consumption of each hourly demand (i.e., d_{itL2} and d_{itL3}) could be calculated based on the power of chargers and dwell time at the destination.

As for accessibility, this study assumed new public charging stations could only be installed at public parking lots due to space and facility requirements. A catchment area with a radius r was created for each public parking lot to quantify the accessibility of drivers to the parking lot. If the driver's current location fell within the catchment area, then, the driver's current charging request was considered to have the potential to be fulfilled by that parking lot (where a charging station can be sited). The last constraint was the investment budget. It was calculated as the sum of assets values of existing charging stations, since we aimed to optimally reallocate existing charging stations. The mathematical formulation of CMCLP is defined as follows:

Objective function:

$$\text{Maximize } \sum_{i\in I}\sum_{t\in T} d_{it}^{L2}\sum_{j\in J_i} z_{itj}^{L2}+\sum_{i\in I}\sum_{t\in T} d_{it}^{L3}\sum_{j\in J_i} z_{itj}^{L3} \quad (2)$$

Subject to:

$$y_j^{L2} + y_j^{L3} \le P_{max}x_j\ , \forall j \in J \quad (3)$$

$$\sum_{j\in J}(C^S x_j + C^{L2}y_j^{L2} + C^{L3}y_j^{L3}) \le P \quad (4)$$

$$\sum_{(i,t)\in\Omega_j} z_{itj}^{L2} \le y_j^{L2}, \forall j \in J, \forall t \in T \quad (5)$$

$$\sum_{(i,t)\in\Omega_j} z_{itj}^{L3} \le y_j^{L3}, \forall j \in J, \forall t \in T \quad (6)$$

$$x_j = \{0,1\}, \forall k \in K \quad (7)$$
$$y_j^{L2} \in \mathbb{N}, \forall j \in J$$
$$y_j^{L3} \in \mathbb{N}, \forall j \in J$$
$$z_{itj}^{L2} = \{0,1\}, \forall i \in I, \forall t \in T, \forall j \in J$$
$$z_{itj}^{L3} = \{0,1\}, \forall j \in I, \forall t \in T, \forall j \in J$$

The objective function (2) maximized the total service of hourly Level 2 and Level 3 charging demands. Constraints (3) guaranteed the total number of standard and fast charging ports should be no more than P_{max} if the charging station was sited at public parking lot *j*. Constraint (4) imposed the total budget limit for installing public charging stations and ports. Constraints (5) and (6) set the hourly capacity for L2 and L3 chargers, separately. For each charging station x_j, the number of standard/fast hourly demanded it covers at each particular hour *t* should be less than the total number of standard/fast charging ports (y_j^{L2}/y_j^{L3}). Constraints (7) impose integer or binary integer restrictions on decision variables.

Table 4.3 Description of input parameters

Input Parameters	Descriptions
i	the index of EVs that have daily charging requests
I	the set of EVs that have daily charging requests
j	the index of public parking lot location
J	the set of public parking lots
t	the index of the hour of the day
T	the set of hours of the day
d_{it}^{L2}	the hourly L2 charging demand (kWh) of vehicle *i* at hour *t*
d_{it}^{L3}	the hourly L3 charging demand (kWh) of vehicle *i* at hour *t*
P	the total investment budget for public charging stations
P_{max}	the maximum number of ports for each charging station
C^S	the cost for installing a single charging station
C^{L2}	the equipment cost for one standard charging port
C^{L3}	the equipment cost for one fast charging port

Table 4.4 Description of decision variables

Decision variables	Descriptions
y_j^{L2}	the number of L2 chargers installed at public parking lot *j*
y_j^{L3}	the number of L3 chargers installed at public parking lot *j*
z_{itj}^{L2}	$\begin{cases} 1 & \text{, if } d_{it}^{L2} \text{ can be satisfied by the charging station at } j \text{ and hour } t \\ 0 & \text{, otherwise} \end{cases}$
z_{itj}^{L3}	$\begin{cases} 1 & \text{, if } d_{it}^{L3} \text{ can be satisfied by the charging station at } j \text{ and hour } t \\ 0 & \text{, otherwise} \end{cases}$
x_j	$\begin{cases} 1 & \text{, if parking lot } j \text{ is used for installing public charging station} \\ 0 & \text{, otherwise} \end{cases}$
Ω_j	the set of (i, t) that can be served by the public parking lot *j*

5. RESULTS AND ANALYSIS

5.1 Case Study

The Salt Lake City (SLC) metropolitan area was used as a case study to demonstrate the framework implementation. SLC metropolitan region covers approximately 940 km2 and includes 407,442 households with about 826,000 vehicles. The entire study area consists of 1090 TAZs. A report from American Driving Survey (Triplett, Santos, Rosenbloom, & Tefft, 2016) indicated 78% of drivers performed at least one driving trip in a day on average. Therefore, it is assumed 644,300 vehicles will be on the road for simulation. In MATSim, a day trip is defined as a round trip starting from home and returning home before midnight. Besides, a day trip can include several intermediate stops (e.g., workplaces, restaurants, etc.) After data processing, 17.4% of trips after location mapping are considered invalid and therefore discarded. The final inputs to MATSim contained 532,460 trips. MATSim takes these planned trips as inputs, and optimizes driving events iteratively based on co-evolutionary principle. In this study, MATSim was executed with 100 iterations. When the iteration time reached 55, the computation was nearly converged. For post-MATSim analysis, road traffic was assumed to consist of light-duty vehicles and EVs.

EV adopters were determined by Eq. (1). The required socioeconomic variables in Eq. (1) for each synthetic driver was known, thus its probability in adopting EV could be calculated. The EV adoption probabilities across TAZs (Figure 5.1) ranged from 0.6% to 21% with a mean value of 4.3%. Correspondingly, among the 532,460 drivers, 22,737 drivers were assigned with EVs. The EV charging profile was implemented using the rule specified in Section 3.4. *EV Assignment and Energy Consumption Model*. The initial SoC was empirically determined by a normal distribution with $\mu = 0.85$ and $\sigma = 0.3$, considering that home charging accounts for over 80% of all charging events (Smart & Schey, 2012). As for other EV parameters, the EVs' battery capacity varied widely, from 17.6 to 100 kWh, depending on the manufacturers and car models. For simplicity, the battery capacity was consistently assumed as 62 kWh (Nissan Leaf S Plus). A fixed energy consumption rate was assumed as 0.3 kWh/mile (Plugin America, 2016).

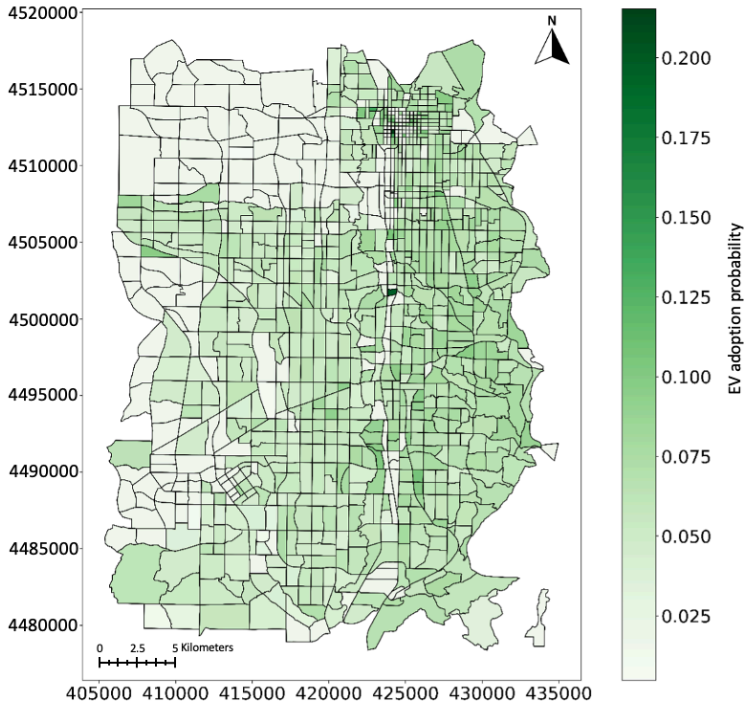

Figure 5.1 The EV adoption probability distribution in SLC metropolitan area. The map is projected and displayed in UTM Zone 12N, with the coordinates' units in meters.

5.2 Stochastic Daily Activities from Markov Chain

Stochastic activities for both light-duty vehicles and EVs were generated from time-inhomogeneous Markov chain, trained using ATUS data. Note that the ATUS data was extracted only for weekdays, since weekends have significantly different activity patterns. Distribution of the proposed six activity states at each time step of a day is displayed in Figure 5.2. Moreover, activity distribution from ATUS was included for comparison.

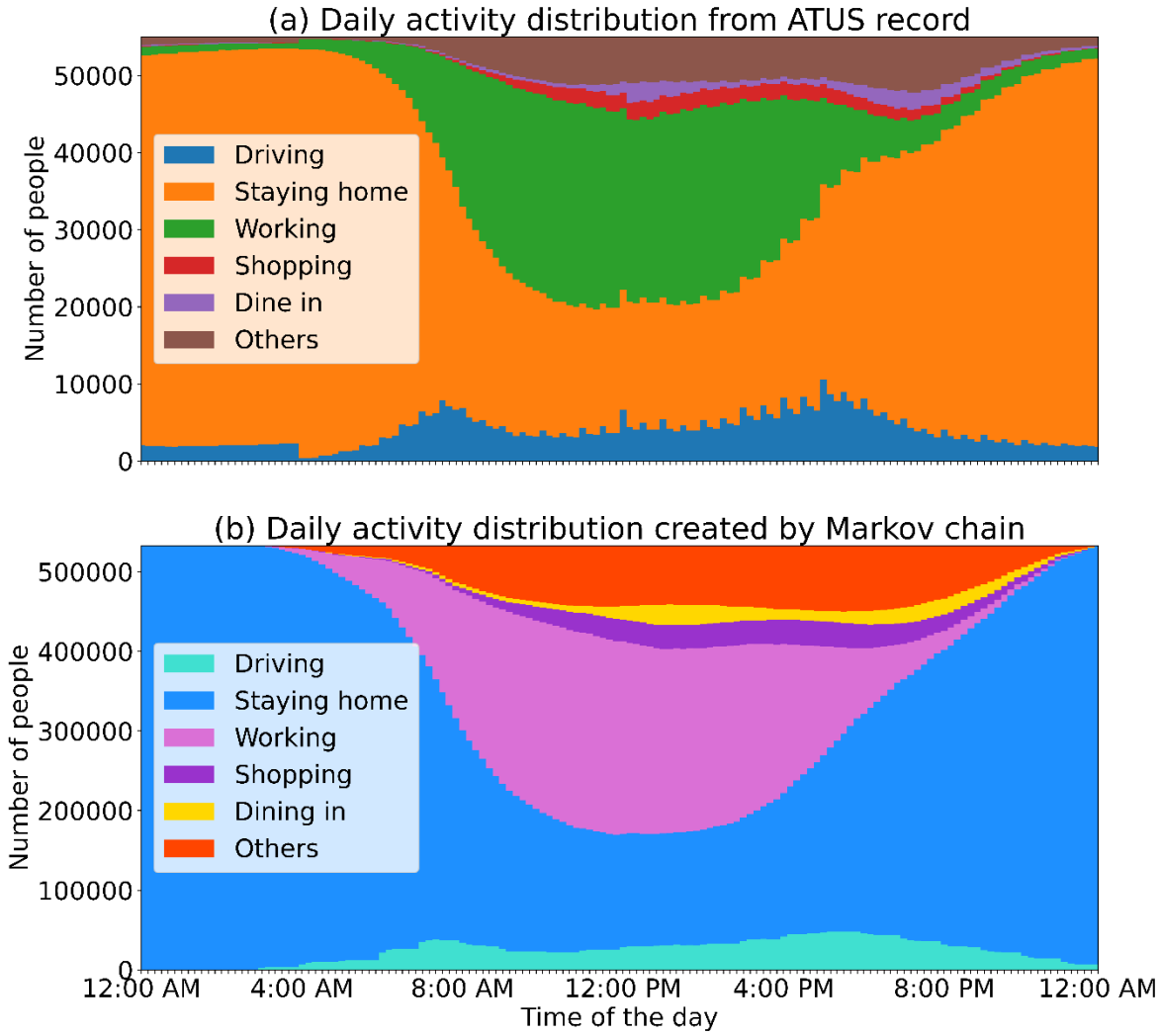

Figure 5.2 A weekday's activity distribution from (a) real-world data; (b) time-inhomogeneous Markov chain

In Figure 5.2, it was found that daily activity distribution from synthetic drivers generated by the Markov chain followed a similar pattern as real-world distribution. During the daytime, the majority of drivers parked their vehicles at workplaces. Apart from work, many drivers also conducted other activities, such as shopping, dining, or entertaining, during the daytime. Several existing studies limit activities for EV users with only staying home, driving, and working states.

As seen from Figure 5.2, such oversimplification can induce biased results by overlooking the impact from nonwork-related activities to public charging. It was also observed that two peaks of traffic flow occured around 8:00 AM and 6:00 PM, respectively. Overall, the simulated daily activities distribution conformed to the reality.

In the next step, daily activities from synthetic drivers were fed into MATSim to perform agent-based simulation onto the road network. MATSim was used to model activities in a single day for agents (i.e., drivers) based on the co-evolutionary principle. During iterations, a certain portion of drivers' plans, such as route and departure time, were modified to search for optimal choices until the entire system reached equilibrium state. The optimized events for those agents from MATSim were an important basis for post-analyses, such as public charging behavior modeling. We first explored the spatial distribution of activities from the MATSim output. Specifically, trip destination count was aggregated by TAZ and compared with real-world historical trip observations as shown in Figure 5.3.

Note that the stochastic daily activity generated by the Markov chain did not contain geolocation information.
The location mapping technique was performed to remedy this. The location mapping process fully utilized POI, road network, and OD information to match the trips within the study region. All trip destinations, including intermediary stops, were aggregated by TAZ in Figure 5.3(a). It was found that the distribution of synthetic trips appeared to be quite similar to the actual trip distribution. Most daily activities were concentrated in the northern part of the study region. The downtown area represents dense trip destinations too, yet the color in those TAZs was relatively light. This was due to the smaller area size of the TAZs within downtown. Note that the total number of actual trip destinations was 2,681,140, while the number of synthetic trip destinations was 2,093,401. Such discrepancy was likely attributable to the filtered 17.4% trips in MATSim. The temporal and spatial analyses sufficiently demonstrated that simulated daily activities were similar to real-world situations. In the next step, analyses related to public charging behaviors was performed to validate against real-world public charging observations.

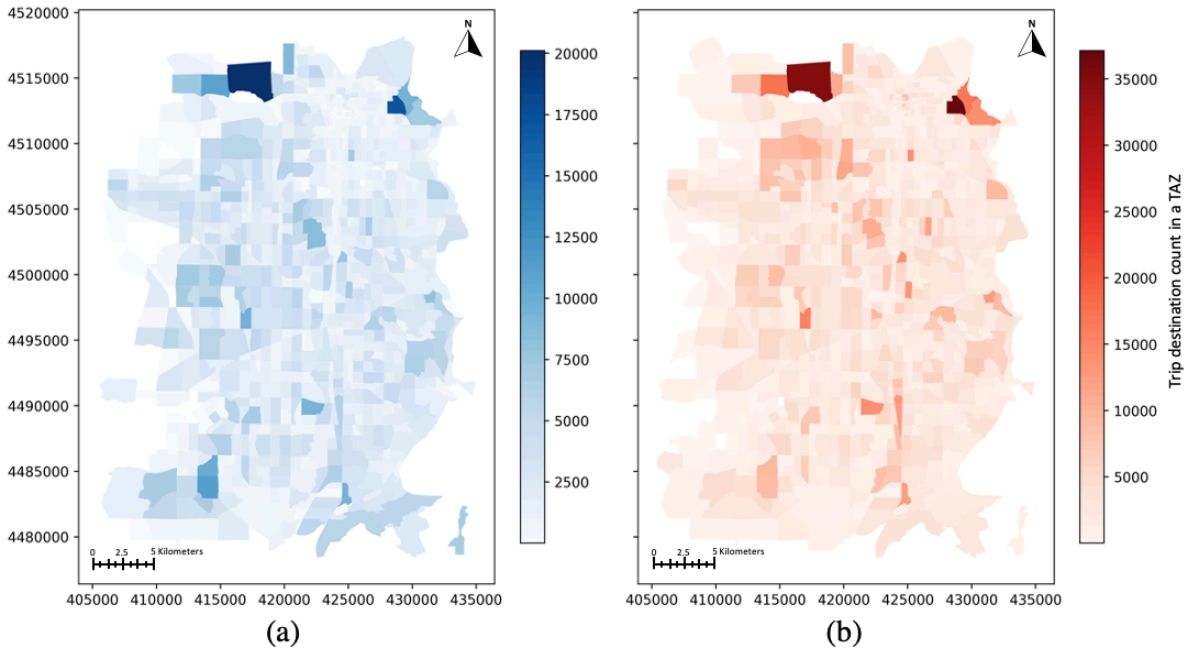

Figure 5.3 The spatial distribution of trip destination: (a) trip destination from simulation and (b) trip destination from real-world data on a typical weekday. The map is projected and displayed in UTM Zone 12N, with the coordinates' units in meters.

5.3 Real-world Public Charging Validation

MATSim output the optimized driving behaviors on a daily basis. Based on the MATSim outputs, EV assignment and charging demand generation were performed as postsimulation offline analysis. The assigned 22,737 EV drivers generated 1,586 charging requests during a day, with 1,366 events belonging to standard charging requests. To compare the estimated public charging demand with real-world observations, the energy data crawled from ChargePoint was averaged by day. Figure 5.4 presents the spatial distribution of estimated public charging demand and actual energy consumption, where the green dots represent public charging stations, and a larger radius indicates higher energy consumption in reality. The background layer shows aggregated estimated charging demand by TAZ with the color representing charging demand density, defined as the summed daily energy request divided by the area of TAZ (kWh/m_2).

In general, it was observed that public charging stations in TAZs with higher estimated charging demand density tended to have higher energy consumption. For instance, SLC downtown (highlighted by blue square) demonstrated both higher public charging demand density and energy consumption. That is likely because TAZs in the downtown area had dense trip destinations and were sited with a large number of POIs related to working, entertaining, and other purposes. Note that the charging stations around the airport (highlighted by red polygon) indicated high usage frequency, while charging demand density was relatively low. This was due to the large area size for that TAZ. On the contrary, TAZs in South Salt Lake County had relatively lower charging demand density due to fewer trip destinations as shown in Figure 5.3. We also noticed that several TAZs with high estimated public charging demand density were not allocated with public charging stations. The proposed charging station location optimization can effectively address this issue. Apart from spatial distribution, temporal trends for public charging station utilization are worthy of exploration. To this end, we selected three TAZs with different levels of energy demand, and compared the estimated daily charging demand at different times-of-the-day with real-world charging station utilization records. The results are presented in Figure 5.5.

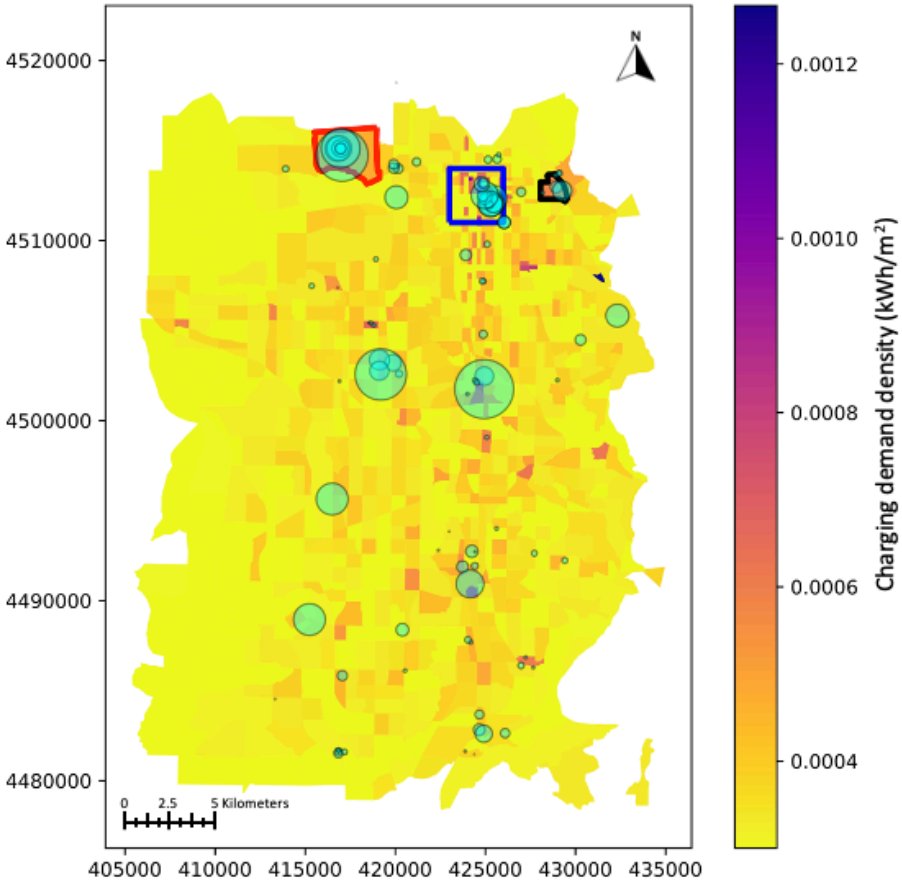

Figure 5.4 Spatial distribution of real-world public charging energy consumption (green circle) and estimated charging demand density by TAZ (background layer). The map is projected and displayed in UTM Zone 12N, with the coordinates' units in meters.

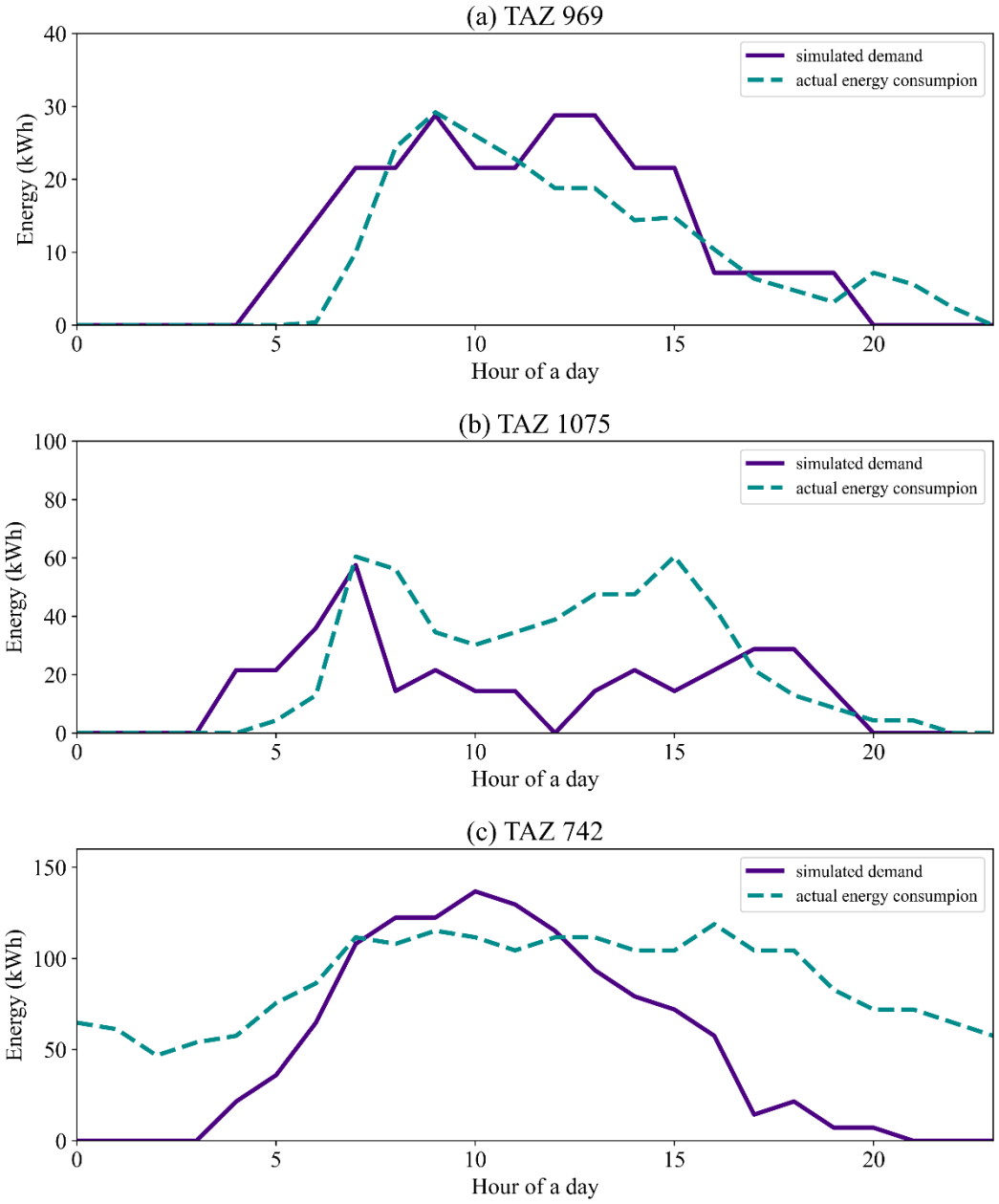

Figure 5.5 Real public charging energy consumption versus simulated public charging demand in representative TAZs

Figure 5.5 compares estimated energy demand and actual energy consumption at the TAZ level in areas that have varying land-use patterns. TAZ 969 is a small block located in SLC downtown. The public charging peaked at around 9:00 AM, and the demand gradually decreased afterwards. Such a charging pattern is generally found in regions with lots of office buildings. Figure 5.5 (b) shows the charging pattern of TAZ 1075, an area in the vicinity of downtown (highlighted by black in Figure 5.4). Although office buildings were not densely located in this TAZ, the University of Utah and University hospital are located in within, serving as major traffic generators. However, the charging pattern was different from that in the downtown area, where two peaks (one around 8:00 AM and one around 3:00 PM for public charging) were found. This can be explained by the fact that some EV drivers did not come to the location

for work. Instead, the drivers could have been students or patients conducting activities other than work. Last, TAZ 742 (highlighted by red in Figure 5.4) included the SLC international airport. Due to the uniqueness of the airport, trip density and public charging, demand were significantly higher than other TAZs as indicated in Figure 5.5(c).

Another distinction for this TAZ was that many EVs were left charging overnight at the airport. However, when estimating the charging demand in our framework, we only considered the potential charging opportunities linked between two activities via driving during the day (e.g., home, work, shopping, etc.) Yet overnight charging was neither modeled nor within the scope of our study. Overall, the daily charging pattern matched actual energy consumption for those selected TAZs without large deviation during the daytime. While the majority of TAZs showed a consistent pattern between the estimated charging demand and actual energy consumption, there were several locations with high estimated charging demand density that had not been assigned any charging station, and locations with charging stations that are significantly underutilized. Another potential problem was that with the increase in EV adoption, public charging demand would increase significantly, which poses challenges to existing charging stations, especially during peak hours in popular regions. For this reason, charging stations should be optimally reallocated such that they can be effectively utilized while avoiding extremely long queues during peak hours in the future. In the following section, we focus on optimizing charging stations considering demand increases in the future.

5.4 Public charging station optimization result

The CMCLP model aims to maximize the coverage of the public charging demand considering charging capacity, access distance, and investment cost. As for the access distance, EV drivers may opt for alternative solutions, such as home charging, if walking distance is beyond 0.91 km, according to (Seneviratne, 1985). For this reason, radius r for the catchment area for each public parking lot was set as 1,000 m. Meanwhile, the investment budget was calculated using the current 109 charging stations with 516 Level 2 ports. In general, the cost of installing a charging station is approximately $5,500, including labor cost and materials, and the average prices for L2 port and L3 port are around $2,500 and $5,500, separately (Borlaug, Salisbury, Gerdes, & Muratori, 2020). The total budget was, therefore, approximated at $1.89 million ($5500*109 + $2500*516). For parameters related to charging stations, Level 2 chargers were uniformly assumed as J1772 plugs with power of 7.2 kW, and Level 3 chargers were uniformly assumed as CHAdeMO plugs with power of 50 kW. The maximum number of ports P_{max} was set as eight for simplicity. In this study, we optimized charging station locations considering charging demand increase in the future. The main purpose of considering demand increase was to handle exponential EV adoption increase. Besides, providing insightful guidance for new charging station deployment in the future, it is of practical use to local agencies to assist with infrastructure planning and decision making.

A report from Bloomberg projected the national EV adoption would reach 12% in 2030 and >50% in 2050 (Ghamami, Zockaie, Wang, & Miller, 2019). Given such projection, scaling factor 3.5 was used to augment EV penetration from 4.3% to 15% as charging demand increases. Subsequently, we estimated such public charging demand according to the designed energy consumption model and charging rules. Upon scaling, 80,182 EVs with 5,820 daily public charging events were identified in SLC metropolitan area — 5,061 were slow charging events and 759 were fast charging events. Here, the CMLCP was solved using a commercial optimization solver Gurobi. Optimized layout is displayed in Figure 5.6.

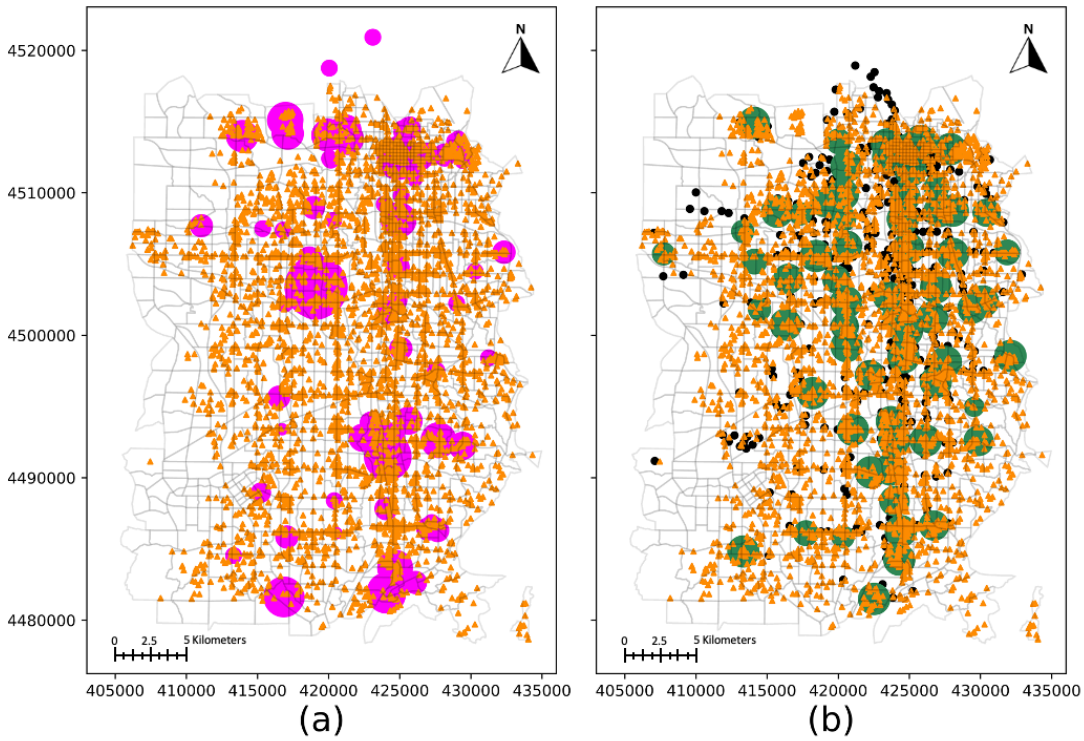

Figure 5.6 Public charging demand distribution and (a) existing layout of public charging stations; (b) optimized layout of public charging stations. The map is projected and displayed in UTM Zone 12N, with the coordinates' units in meters.

The orange triangles in Figure 5.6 (a) and (b) denote estimated public charging demand. The black dots in Figure 5.6 (b) represent available public parking lots that can be used to build charging stations. The magenta circles in Figure 5.6 (a) and green circles in Figure 5.6 (b) are current and optimized charging stations, respectively, with a radius representing the number of chargers. After optimization, the original 109 charging stations (516 Level 2 ports) were transformed to 64 charging stations with 313 Level 2 ports and 136 Level 3 ports reallocated throughout the region. Although fast charging demands only accounted for 13% of total demands, 30% chargers were Level 3 after optimization. Level 3 charging can provide full miles of range within an hour, which satisfy public charging need in a shorter time when drivers conduct short-duration activities other than work. It was observed that public charging stations were densely congregated in SLC downtown area both before and after optimization due to the large amount of public charging demand. Overall, public charging stations were mostly reallocated in the northern part of SLC metropolitan area after optimization, most likely due to the concentration of outdoor activities. The southern area has fewer public parking lots that allow for new charging stations siting.

One issue with the optimization was several spots with significant charging demands were not assigned with charging stations, such as the airport, due to the unavailability of public parking lots. However, commercial buildings may be used to build charging stations to replace public parking lots for future deployment. The CMCLP solution presents an optimized reallocated charging station layout. In practice, future EVSE deployment should be considered upon existing charging stations. As such, we evaluated the overall utilization between existing charging stations and optimized stations. Specifically, we split existing charging stations into two groups — charging stations that are overlapped with optimized charging stations (group 1) and charging stations that are not overlapped with optimized charging stations (group 2). For optimized results, we also split them into two groups — charging stations that are

overlapped with existing charging stations (group 3) and charging stations that should be newly installed (group 4). For groups 1 and 3, overlapping is defined as the distance between two stations being <1 km. To observe the utilization efficiency for each group of charging stations, we assigned each charging request to the nearest station within the walk distance (1 km) and aggregated the number of charging requests by maximum, mean, and minimum. The charging requests assignment were performed for existing layout and optimized layout, separately. Table 5.1 shows the basic charging station information and the utilization status for each group.

Table 5.1 Utilization comparison between existing stations and optimized stations

	Existing layout		Optimized layout	
	Group 1	Group 2	Group 3	Group 4
Station count	30	79	30	34
Port count	112	404	213	236
Slow charging port	112	404	151	162
Fast charging port	NA	NA	62	74
Min. requests covered	21	0	23	20
Avg. requests covered	45.0	15.5	46.8	40.7
Max. requests covered	110	59	120	72

In Table 5.1, it can be observed that the optimized layout had a higher coverage rate than existing charging stations. Specifically, group 2 presented extremely low coverage with 15.5 times per day on average. Existing charging stations in group 2 were mostly distributed in remote areas or in the vicinity of dense clusters. One practical guidance for future EVSE installation is to keep maintaining those overlapped charging stations (group 1) and moderately adjust the number and type of charging ports. For those underutilized charging stations (group 2), we should reallocate them to new areas to fulfill higher (or new) charging demands. To validate that the optimized public charging stations layout could provide more effective charging utilization, UrbanEV-Contrib was applied to simulate public charging behavior in MATSim.

UrbanEV-Contrib is an open-source framework capable of performing high-resolution analysis of urban electric mobility based on MATSim — and serve as a MATSim plug-in module (Adenaw & Lienkamp, 2021). By inputting charging configurations and rules, UrbanEV-Contrib returns charging states and events in time series, which serves as a sandbox validating charging infrastructure design on the city-scale. To compare charging effectiveness, MATSim was reperformed with scaled EV drivers and corresponding public charging requests. Existing charging stations and optimized charging stations were inserted into the simulation environment separately to satisfy those charging requests using UrbanEV-Contrib plug-in. The remaining SoCs was one important metric to reflect the effectiveness of public charging station deployment, since a high level of SoC values after completing a series of daily activities denotes that charging station locations can be easily accessed by EV drivers while they conduct other activities. For this reason, remaining SoCs were examined upon completion of people's daily activities under two different scenarios in Figure 5.7.

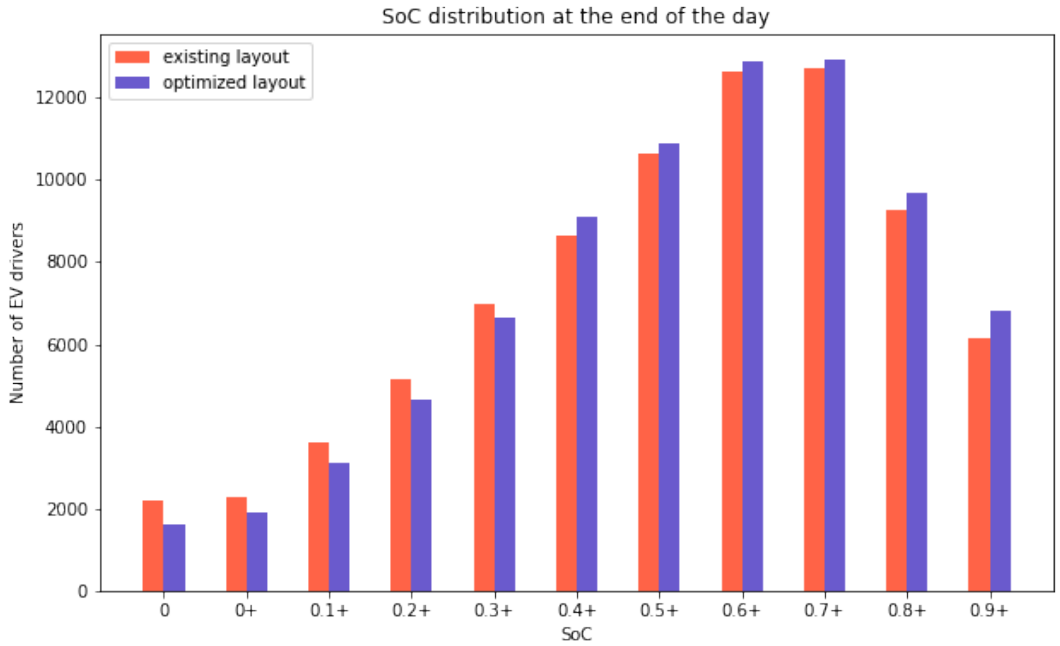

Figure 5.7 SoC distribution after daily stochastic activities

The first column in Figure 5.7 denotes drivers who consumed all EV energy after completing a series of daily activities. While it is not realistic to exhaust SoC entirely, it was an important metric to evaluate how many drivers failed to access public charging stations during their daily activities. Overall, the number of drivers with 0 SoCs by the end of the day decreased by 20% as a result of charging station optimization. When SoC is too low, drivers may have range anxiety. The optimized layout effectively decreased the number of drivers with low SoC values to ensure higher accessibility and reduce range anxiety.

It is also noted that the number of drivers with high SoC values increased to some extent. Higher values of SoC at the end of the day indicated optimized charging stations make longer trips feasible for more EV drivers. In the next step, we explored the temporal profile of charging station occupancy. The number of chargers in use at different hours-of-the-day are plotted in Figure 5.8.

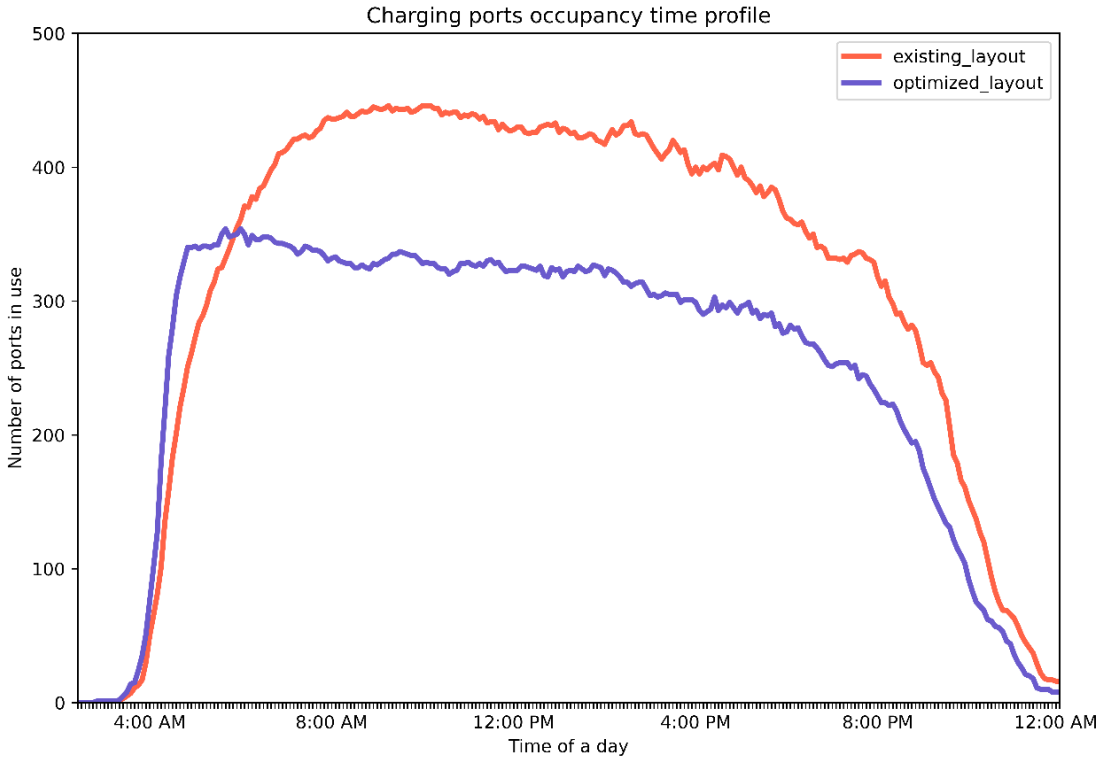

Figure 5.8 The time profile of charger occupancy

Figure 5.8 shows a temporal shift of charger occupancy peak in the optimized scenario. One possible explanation was charging stations are more easily accessed after optimization. It was observed that the number of charging ports occupied during the day (8:00 AM to 3:00 PM) became less upon optimization. This was due to the fact of more Level 3 charging stations, enabling drivers to charge with a shorter time. With the current layout of charging stations, the average charging time was 2.8 h, while the charging time was reduced to 2.5 h on average after optimization. Moreover, the optimized layout allowed EV drivers to access charging stations with shorter walking distances. The average walking distance was reduced from 310 m to 270 m, providing drivers with more convenience.

6. CONCLUSION

This study presented an urban-scale public charging station location optimization framework through microscopic modeling. The modeling process followed the classical two-step approach (i.e. public charging demand simulation and charging station location optimization). One major highlight was that the presented methodology addressed the oversimplification and limitations constrained in previous literature by utilizing high-fidelity city-scale road network, incorporating drivers' non-work-based activities, and applying real-world EV distribution to develop a charging demand estimation model.

Also, most existing studies failed to validate their proposed models due to the difficulty of retrieving real-world charging event records. As such, another novelty of this research was the availability of real-work public charging events, which proved the validity of our modeling results. On top of the reliable simulation, we performed the CMCLP model to reallocate existing charging stations with the objective of maximizing the coverage of charging demand. The optimization model incorporated practical constraints, such as walking accessibility and different charging modes. The optimized deployment scheme can provide meaningful guidance for Salt Lake City metropolitan areas and many alike.

We implemented our methodological pipeline onto Salt Lake City metropolitan area to showcase the effectiveness. A series of validations were conducted to justify the robustness of simulation results. Specifically, the temporal and spatial distributions of drivers' daily activities were validated against ATUS data and historical OD data, respectively. Numerical results showed the time-inhomogeneous Markov chain with the proposed location mapping technique could be effectively used for trip generation, which is highly generalizable and replicable to other regions. Moreover, real-world public charging records were used to validate the spatiotemporal distribution of the synthetic public charging demands. It was found that the majority of TAZs demonstrated a consistent pattern between the estimated charging demand and actual energy consumption. Once the fidelity of simulation results was guaranteed, we applied CMCLP optimization model with 15% EV penetration rate to account for the potential charging demand increase in the future. We further incorporated the plug-in UrbanEV-Contrib to perform agent-based simulation under the public charging context. It was found that the optimized layout could improve overall charging performance by decreasing the number of drivers with 0 SoCs by the end of the day over 20% and reducing the average charging time from 2.8 h to 2.5 h.

6.1 Implications and Improvements

The simulation experimental results offered meaningful political implications for governmental agencies. First, the existing coverage of fast charging stations in SLC metropolitan area was highly insufficient. Although the financial constraint was a major concern for building Level 3 chargers, agencies should still incentivize the fast-charging station deployment, since it is a critical step moving toward accelerated EV adoption and reaching net-zero emission goal by 2050. Second, low utility efficiency was identified at a lot of existing charging stations with extremely large number of ports and/or clustered densely in close vicinity. Instead, a decentralized design could effectively augment EV drivers' accessibility to the nearest charging stations. Last, some atypical activities could also impact public charging demand. Places, such as airport and stadium, are examples of locations where large charging demand could exist due to atypical activities. This study was confined to investigating intracity travels (i.e. trips within the city), and intercity travels (i.e. trips that traverse multiple cities) were not within the scope. For those distant trips, EV drivers were more subject to range anxiety. Deploying fast chargers by identifying critical links or connection points for long-distance travels is worthy of exploration for future study.

REFERENCES

Adenaw, L., & Lienkamp, M. (2021). Multi-criteria, co-evolutionary charging behavior: An agent-based simulation of urban electromobility. World Electric Vehicle Journal, 12(1), 1–26. https://doi.org/10.3390/wevj12010018

Asamer, J., Reinthaler, M., Ruthmair, M., Straub, M., & Puchinger, J. (2016). Optimizing charging station locations for urban taxi providers. Transportation Research Part A: Policy and Practice, 85, 233–246. https://doi.org/10.1016/j.tra.2016.01.014

Axhausen, W., Horni, A., & Nagel, K. (2016). The multi-agent transport simulation MATSim. Ubiquity Press.

Boeing, G. (2017). OSMnx: New methods for acquiring, constructing, analyzing, and visualizing complex street networks. Computers, Environment and Urban Systems, 65, 126–139. https://doi.org/10.1016/j.compenvurbsys.2017.05.004

Bor´en, S., Nurhadi, L., Ny, H., Rob`ert, K. H., Broman, G., & Trygg, L. (2017). A strategic approach to sustainable transport system development - part 2: The case of a vision for electric vehicle systems in Southeast Sweden. Journal of Cleaner Production, 140, 62–71. https://doi.org/10.1016/j.jclepro.2016.02.055

Borlaug, B., Salisbury, S., Gerdes, M., & Muratori, M. (2020). Levelized cost of charging electric vehicles in the United States. Joule, 4(7), 1470–1485. https://doi.org/10.1016/j.joule.2020.05.013

Charge Point. (2021). https://na.chargepoint.com/charge_point.

Church, R., & ReVelle, C. (1974). The maximal covering location problem. Papers of the Regional Science Association, 32(1), 101–118.

Deb, S., Kalita, K., & Mahanta, P. (2018). Impact of electric vehicle charging stations on reliability of distribution network. In Proceedings of 2017 IEEE international conference on technological advancements in power and energy: Exploring energy solutions for an intelligent power grid, TAP energy 2017, 1 (pp. 1–6). https://doi.org/ 10.1109/TAPENERGY.2017.8397272

Deb, S., Tammi, K., Kalita, K., & Mahanta, P. (2018). Review of recent trends in charging infrastructure planning for electric vehicles. Wiley Interdisciplinary Reviews: Energy and Environment, 7(6), 1–26. https://doi.org/10.1002/wene.306

Debnath, R., Bardhan, R., Reiner, D. M., & Miller, J. R. (2021). Political, economic, social, technological, legal and environmental dimensions of electric vehicle adoption in the United States: A social-media interaction analysis. Renewable and Sustainable Energy Reviews, 152(September), Article 111707. https://doi.org/ 10.1016/j.rser.2021.111707

Dong, G., Ma, J., Wei, R., & Haycox, J. (2019). Electric vehicle charging point placement optimisation by exploiting spatial statistics and maximal coverage location models. Transportation Research Part D: Transport and Environment, 67(November 2018), 77–88. https://doi.org/10.1016/j.trd.2018.11.005

Ghamami, M., Zockaie, A., Wang, J., & Miller, S. (2019). Electric vehicle charger placement optimization in Michigan: Phase I-highways (supplement I: Full tourism analysis). March https://www.michigan.gov/documents/energy/Tourism-Supplem entaryReport_662002_7.pdf.

Google Place API. (2021). https://developers.google.com/maps/documentation/places/web-service/search.

Hakimi, S. L. (1964). Optimum locations of switching centers and the absolute centers and medians of a graph. Operations Research, 12(3), 450–459.

He, F., Yin, Y., & Zhou, J. (2015). Deploying public charging stations for electric vehicles on urban road networks. Transportation Research Part C: Emerging Technologies, 60, 227–240. https://doi.org/10.1016/j.trc.2015.08.018

Herberz, M., Hahnel, U. J. J., & Brosch, T. (2022). Counteracting electric vehicle range concern with a scalable behavioural intervention. Nature Energy, 1–8.

Hodgson, M. J. (1990). A flow-capturing location-allocation model. Geographical Analysis, 22(3), 270–279.

Hu, L., Dong, J., Lin, Z., & Yang, J. (2018). Analyzing battery electric vehicle feasibility from taxi travel patterns: The case study of new York City, USA. Transportation Research Part C: Emerging Technologies, 87(April 2017), 91–104. https://doi.org/10.1016/j.trc.2017.12.017

Huang, K., Kanaroglou, P., & Zhang, X. (2016). The design of electric vehicle charging network. Transportation Research Part D: Transport and Environment, 49, 1–17. https://doi.org/10.1016/j.trd.2016.08.028

Javid, R. J., & Nejat, A. (2017). A comprehensive model of regional electric vehicle adoption and penetration. Transport Policy, 54(November 2016), 30–42. https://doi.org/10.1016/j.tranpol.2016.11.003

Khan, S. U., Mehmood, K. K., Haider, Z. M., Rafique, M. K., & Kim, C. H. (2018). A bilevel EV aggregator coordination scheme for load variance minimization with renewable energy penetration adaptability. Energies, 11(10). https://doi.org/10.3390/en11102809

Kontou, E., Liu, C., Xie, F., Wu, X., & Lin, Z. (2019). Understanding the linkage between electric vehicle charging network coverage and charging opportunity using GPS travel data. Transportation Research Part C: Emerging Technologies, 98(November 2017), 1–13. https://doi.org/10.1016/j.trc.2018.11.008

Krajzewicz, D., Erdmann, J., Behrisch, M., & Bieker, L. (2012). Recent development and applications of SUMO-simulation of urban MObility. International Journal on Advances in Systems and Measurements, 5(3&4).

Kumar, R. R., Chakraborty, A., & Mandal, P. (2021). Promoting electric vehicle adoption: Who should invest in charging infrastructure? Transportation Research Part E: Logistics and Transportation Review, 149(April), Article 102295. https://doi.org/10.1016/j.tre.2021.102295

Liu, X., Sun, X., Zheng, H., & Huang, D. (2021). Do policy incentives drive electric vehicle adoption? Evidence from China. Transportation Research Part A: Policy and Practice, 150(May), 49–62. https://doi.org/10.1016/j.tra.2021.05.013

Lopez, N. S., Allana, A., & Biona, J. B. M. (2021). Modeling electric vehicle charging demand with the effect of increasing evses: A discrete event simulation-based model. Energies, 14(13), 1–15. https://doi.org/10.3390/en14133734

Macal, C. M., & North, M. J. (2009). Agent-based modeling and simulation. In Proceedings of the 2009 winter simulation conference (WSC) (pp. 86–98).

Maciejewski, M., & Nagal, K. (2007). Simulation and dynamic optimization of taxi services in MATSim. Europe, 79, 21. https://doi.org/10.1287/xxxx.0000.0000

Marmaras, C., Xydas, E., & Cipcigan, L. (2017). Simulation of electric vehicle driver behaviour in road transport and electric power networks. Transportation Research Part C: Emerging Technologies, 80, 239–256. https://doi.org/10.1016/j.trc.2017.05.004

McKinsey. (2019). Expanding electric - vehicle adoption despite early growing pains. McKinsey & Company, August.

Nansai, K., Tohno, S., Kono, M., Kasahara, M., & Moriguchi, Y. (2001). Life-cycle analysis of charging infrastructure for electric vehicles. Applied Energy, 70(3), 251–265. https://doi.org/10.1016/S0306-2619(01)00032-0

US Department of Energy. (2022). New Plug-in Electric Vehicle Sales. https://www.energy.gov/energysaver/articles/new-plug-electric-vehicle-sales-united-states-nearlydoubled-2020-2021, 2022.

Novosel, T., Perkovi´c, L., Ban, M., Keko, H., Puk˘sec, T., Kraja˘ci´c, G., & Dui´c, N. (2015). Agent based modelling and energy planning - utilization of MATSim for transport energy demand modelling. Energy, 92, 466–475. https://doi.org/10.1016/j.energy.2015.05.091

Ou, S., Lin, Z., He, X., & Przesmitzki, S. (2018). Estimation of vehicle home parking availability in China and quantification of its potential impacts on plug-in electric vehicle ownership cost. Transport Policy, 68(April), 107–117. https://doi.org/10.1016/j.tranpol.2018.04.014

Paoli, L., & Gül, T. (2022). Electric cars fend off supply challenges to more than double global sales.

Paul, B. M., Doyle, J., Stabler, B., Freedman, J., & Bettinardi, A. (2018). Multi-level population synthesis using entropy maximization-based simultaneous list balancing. Transportation Research Board 93rd Annual Meeting. January 12-16, Washington, D.C. (Vol. 4457(785), pp. 1–19)

Plugin America. (2016). https://pluginamerica.org/how-much-does-it-cost-charge-electric-car/.

Seneviratne, P. N. (1985). Acceptable walking distances in central areas. Journal of Transportation Engineering, 111(4), 365–376.

Sheppard, C., Waraich, R., Campbell, A., Pozdnukov, A., & Gopal, A. R. (2017). Modeling plug-in electric vehicle charging demand with BEAM: The framework for behavior energy autonomy mobility. In Lawrence Berkeley national lab. Berkeley, CA (United States): LBNL.

Smart, J., & Schey, S. (2012). Battery electric vehicle driving and charging behavior observed early in the EV project. SAE Technical Papers, 1(1), 27–33. https://doi.org/10.4271/2012-01-0199

Smith, L., Beckman, R., & Baggerly, K. (1995). TRANSIMS: Transportation analysis and simulation system.

Triplett, T., Santos, R., Rosenbloom, S., & Tefft, B. (2016). American driving survey 2014–2015. American Driving Survey. September, 2014–2015 www.aaafoundation.org.

Tu, W., Li, Q., Fang, Z., Shaw, S. L., Zhou, B., & Chang, X. (2016). Optimizing the locations of electric taxi charging stations: A spatial–temporal demand coverage approach. Transportation Research Part C: Emerging Technologies, 65(3688), 172–189. https://doi.org/10.1016/j.trc.2015.10.004

United States Census Bureau. (2019). https://www.census.gov/programs-surveys/acs/microdata.html.

Vazifeh, M. M., Zhang, H., Santi, P., & Ratti, C. (2019). Optimizing the deployment of electric vehicle charging stations using pervasive mobility data. Transportation Research Part A: Policy and Practice, 121(September 2018), 75–91. https://doi.org/10.1016/j.tra.2019.01.002

Wang, K., & Ke, Y. (2018). Public-private partnerships in the electric vehicle charging infrastructure in China: An illustrative case study. Advances in Civil Engineering, 2018. https://doi.org/10.1155/2018/9061647

Wang, Y., Huang, S., & Infield, D. (2014). Investigation of the potential for electric vehicles to support the domestic peak load. In 2014 IEEE international electric vehicle conference, IEVC 2014. https://doi.org/10.1109/IEVC.2014.7056124

Wang, Y., & Infield, D. (2018). Markov chain Monte Carlo simulation of electric vehicle use for network integration studies. International Journal of Electrical Power & Energy Systems, 99(March 2017), 85–94. https://doi.org/10.1016/j.ijepes.2018.01.008

Wasatch Front Regional Council. (2021). http://wfrc.org.

Wu, Y., Ravey, A., Chrenko, D., & Miraoui, A. (2019). Demand side energy management of EV charging stations by approximate dynamic programming. Energy Conversion and Management, 196(April), 878–890. https://doi.org/10.1016/j.enconman.2019.06.058

Xi, X., Sioshansi, R., & Marano, V. (2013). Simulation-optimization model for location of a public electric vehicle charging infrastructure. Transportation Research Part D: Transport and Environment, 22, 60–69. https://doi.org/10.1016/j.trd.2013.02.014

Yang, J., Dong, J., & Hu, L. (2018). Design government incentive schemes for promoting electric taxis in China. Energy Policy, 115(2), 1–11. https://doi.org/10.1016/j.enpol.2017.12.030

Yi, Z., Liu, X. C., & Wei, R. (2022). Electric vehicle demand estimation and charging station allocation using urban informatics. Transportation Research Part D: Transport and Environment, 106(April), Article 103264. https://doi.org/10.1016/j.trd.2022.103264

Yi, Z., Liu, X. C., Wei, R., Chen, X., & Dai, J. (2021). Electric vehicle charging demand forecasting using deep learning model. Journal of Intelligent Transportation Systems,1–14.

Yi, Z., & Bauer, P. H. (2016). Optimization models for placement of an energy-aware electric vehicle charging infrastructure. Transportation Research Part E: Logistics and Transportation Review, 91, 227–244. https://doi.org/10.1016/j.tre.2016.04.013

Zhang, Y., Luo, X., Qiu, Y., & Fu, Y. (2022). Understanding the generation mechanism of BEV drivers' charging demand: An exploration of the relationship between charging choice and complexity of trip chaining patterns. Transportation Research Part A: Policy and Practice, 158(March), 110–126. https://doi.org/10.1016/j.tra.2022.02.007

Zheng, J., Wang, X., Men, K., Zhu, C., & Zhu, S. (2013). Aggregation model-based optimization for electric vehicle charging strategy. IEEE Transactions on Smart Grid, 4 (2), 1058–1066. https://doi.org/10.1109/TSG.2013.2242207

Zou, Y., Wei, S., Sun, F., Hu, X., & Shiao, Y. (2016). Large-scale deployment of electric taxis in Beijing: A real-world analysis. Energy, 100, 25–39. https://doi.org/10.1016/j.energy.2016.01.062